Predicted Role of NAD Utilization in the Control of Circadian Rhythms During DNA Damage Response

Authors and Affiliations

Augustin Luna[1,2], Geoffrey McFadden[3], Mirit I. Aladjem[1], and Kurt W. Kohn[1]

[1] Laboratory of Molecular Pharmacology, National Cancer Institute, Bethesda, MD, USA

[2] Department of Bioinformatics, Boston University, Boston, MA, USA

[3] Applied and Computational Mathematics Division, National Institute of Standards and Technology, Gaithersburg, MD, USA

Abstract

The circadian clock is a set of regulatory steps that oscillate with a period of approximately 24 hours influencing many biological processes. These oscillations are robust to external stresses, and in the case of genotoxic stress (i.e. DNA damage), the circadian clock responds through phase shifting with primarily phase advancements. The effect of DNA damage on circadian clock and the mechanism through which this effect operates remains to be thoroughly investigated. Here we build an *in silico* model to examine the observed behavior by investigating a possible mechanism building on evidence linking circadian rhythms to metabolism. The proposed mechanism involves two DNA damage response proteins SIRT1 and PARP1 that are each consumers of nicotinamide adenine dinucleotide (NAD), a metabolite involved in oxidation-reduction reactions and in ATP synthesis. This model builds on findings that show that SIRT1 (a protein deacetylase) is involved in both the positive (i.e. transcriptional activation) and negative (i.e. transcriptional repression) arms of the circadian regulation and that PARP1 is a major consumer of NAD during DNA damage response. In our simulation, we observe that increased PARP1 activity may be able to trigger the observed phase advancements by downregulating SIRT1 activity through its competition for NAD supplies. We show how this mechanism may operate through acetylation events in conjunction with phosphorylation events that have also been predicted to be involved in the observed behavior. These findings suggest a possible mechanism through which multiple perturbations each dominant during different points of the circadian cycle may account for the observed behavior resulting in the primarily phase advancement response seen during DNA damage perturbations of the circadian clock.

Introduction

Circadian rhythms and cancer

Circadian rhythms are biological oscillations occurring with an approximately 24 hour period affecting many processes. In mammals, these oscillations are centrally controlled in the brain by the suprachiasmatic nuclei (SCN). The SCN synchronizes the peripheral circadian clocks that exist in nearly every cell. Disruption of the circadian clock can lead to higher incidence of certain forms of cancer, and circadian timing can affect both the tolerability and efficacy of cancer therapeutics though the underlying mechanisms for these effects are still not well-understood (Levi, Okyar et al. 2010; Leonardi, Rapisarda et al. 2012). There is evidence that mutations of core circadian components in tumors can affect several properties of circadian oscillations, including: changes in amplitude, phase shifts, and period (Mormont and Levi 1997).

Circadian mechanism

Investigation into the molecular components of the circadian clock has revealed much about how these biological rhythms function. In mammals, the core of the circadian clock is coordinated by four components that operate in a transcription-translational feedback loop. The positive arm of the circadian clock involves a transactivating heterodimer complex composed of Brain and Muscle Arnt-Like protein-1 (BMAL1) and Circadian Locomotor Output Cycles Kaput (CLOCK) that induces the transcription of many genes; the current model and its simplifications are described in the Model section. Gene expression microarray analyses have shown that as much as 10% of an organism's transcriptome could be under circadian influence with expression exhibiting circadian oscillations; this value is dependent on experimental conditions and the tissue of origin (Ptitsyn and Gimble 2011). The BMAL1/CLOCK transactivating complex operates on E-box regions of gene promoters. Additionally, CLOCK is an acetyltransferase involved in chromatin remodeling; a function necessary to the proper operation of the circadian clock mechanism (Doi, Hirayama et al. 2006). The negative arm of the circadian clock involves the Cryptochrome (CRY1 and CRY2) and Period (PER1, PER2, and PER3) genes that act as inhibitors of the BMAL1/CLOCK transcription factor complex. CRY/PER heterodimers in the nucleus suppress CLOCK/BMAL1-mediated transcription completing the feedback loop, which then repeats as the levels of CRY/PER complex diminish (Reppert and Weaver 2001). The degradation of CRY/PER levels is partially triggered by phosphorylation, which marks the PER proteins for proteasomal degradation (Eide, Woolf et al. 2005). This phosphorylation of the PER occurs via CKI-epsilon (Casein Kinase I-epsilon). There is also evidence that period (PER) proteins have been shown to interact with ATM and CHK2 two key proteins involved in DNA damage response; the *Neurospora* ortholog for CHK2, PRD-4, has been shown to promote the phosphorylation of the PER protein analogue in *Neurospora*, FRQ (Gery, Komatsu et al. 2006; Pregueiro, Liu et al. 2006).

Circadian rhythms, DNA damage response, and metabolism

Several studies show the existence of interplay between the pathways regulating circadian rhythms and those regulating DNA damage response. For example, disruptions to the core components can lead to alterations in DNA damage response pathways through altered expression patterns; reviewed by Rana and Mahmood (Rana and Mahmood 2010). The reverse has also been shown to be the case, in that circadian oscillations can be reset in the presence of genotoxic stress (Oklejewicz, Destici et al. 2008; Engelen, Janssens et al. 2013). In Oklejewicz et al., Rat-1 fibroblasts were subjected to 2-hour treatments of ionizing radiation resulting primarily in phase advancements of circadian oscillations. Other forms of perturbation produce phase advancements and delays, such as in the case of pharmacological perturbation with dexamethasone (Izumo, Sato et al. 2006). Dexamethasone is a glucocorticoid agonist capable of resetting the circadian phase of asynchronous cells by triggering the expression of PER1 (Reddy, Maywood et al. 2007).

The molecular basis for the regulation of the circadian clock in the presence of genotoxic stress continues to be explored (Oklejewicz, Destici et al. 2008; Engelen, Janssens et al. 2013). As our understanding of circadian regulation expands, so do the interconnections with other biological processes. Several recent studies have shown the circadian clock to be regulated by proteins,

such as SIRT1, involved with DNA damage response and cellular metabolic state through their consumption of nicotinamide adenine dinucleotide (NAD) (Nakahata, Kaluzova et al. 2008; Nakahata, Sahar et al. 2009). Supplies of NAD are under circadian regulation due to circadian oscillation of nicotinamide phosphoribosyltransferase (NAMPT) that controls a rate-limiting step in the salvage of NAD (Nakahata, Sahar et al. 2009; Ramsey, Yoshino et al. 2009). NAD is a well-known metabolite that participates in many oxidation-reduction reactions and functions, including ATP production (Rongvaux, Andris et al. 2003).

In its DNA damage response role, NAD is involved in cell fate decisions through its utilization by PARP1 and SIRT1. PARP1 is ADP-ribosyltransferase where the ADP-ribosyl moieties are obtained from the cleavage of NAD. PARP1 is activated in the presence of DNA strand breaks (its activity can increase 10-500 fold) and helps to recruit DNA repair proteins (de Murcia, Niedergang et al. 1997; D'Amours, Desnoyers et al. 1999). At severe levels of DNA damage, energy depletion due to loss of NAD and ATP may trigger necrosis rather than apoptosis (D'Amours, Desnoyers et al. 1999; Koh, Dawson et al. 2005).

SIRT1 is a protein deacetylase that can help regulate transcription through histone deacetylation and is involved in DNA damage response through interaction with several key proteins, such as p53, where the deacetylation of p53 inhibits p53 and promotes cell survival (Kwon and Ott 2008). More recently, SIRT1 has been implicated in the regulation of the circadian clock in several ways. First, SIRT1 destabilizes the interaction between CRY and BMAL1 through the deacetylation of BMAL1; the deacetylation of BMAL1 is counter-balanced at the same position through the acetyltransferase activity of CLOCK (Hirayama, Sahar et al. 2007; Nakahata, Kaluzova et al. 2008). Second, SIRT1 has been shown to deacetylate PER destabilizing the protein and promoting its degradation (Asher, Gatfield et al. 2008). Finally, SIRT1 is recruited to promoters of PER2 and NAMPT and is involved in the chromatin remodeling of the vicinity of each of the two promoters (Nakahata, Sahar et al. 2009).

Current study

The circadian clock has been the subject of several mathematical models that have helped in our understanding of the molecular mechanisms underlying regulation of the circadian clock (Gonze, Halloy et al. 2002; Gallego, Eide et al. 2006). Our understanding of the NAD circadian regulation dynamics and the molecular mechanism regulating the phase resetting response of the circadian clock upon exposure to genotoxic stress remains incomplete; given the interactions mentioned above, there is the possibility that NAD utilization may be involved. We have developed an ordinary differential equation (ODE) model that includes the role of NAD in the regulation of SIRT1. The current study explores the potential role of NAD depletion in phase resetting of the circadian clock through the activities of the NAD consumers, SIRT1 and PARP1. Our study explores the dynamics of NAD depletion on the circadian rhythms. Also, we examine the effect of multiple perturbations on the circadian cycle and how these multiple perturbations may account for this observed behavior of the primarily phase advancement phase resetting response seen during DNA damage perturbations of the circadian clock.

Methods

Model

We have developed a simple model (referred to here as the current model) representing the circadian clock of mammals, which extends a previous model developed by Hong et al. (referred to here as the Hong 2009 model) (Hong, Zámborszky et al. 2009). As in the Hong 2009, we only consider the activity of the PER protein and have subsumed the paralogs of the CRY (Cryptochrome) and PER (Period) genes into a single species CP in order to simplify the model. Within the model, PER can exist as a monomer, dimer, or in complex with BMAL1/CLOCK. BMAL1/CLOCK is inactivated when it exists in a complex with the PER dimer. Each form of PER contains a phosphorylation term that simulates the phosphorylation that triggers proteasomal degradation (Eide, Woolf et al. 2005).

Title: SIRT1/Circadian Model

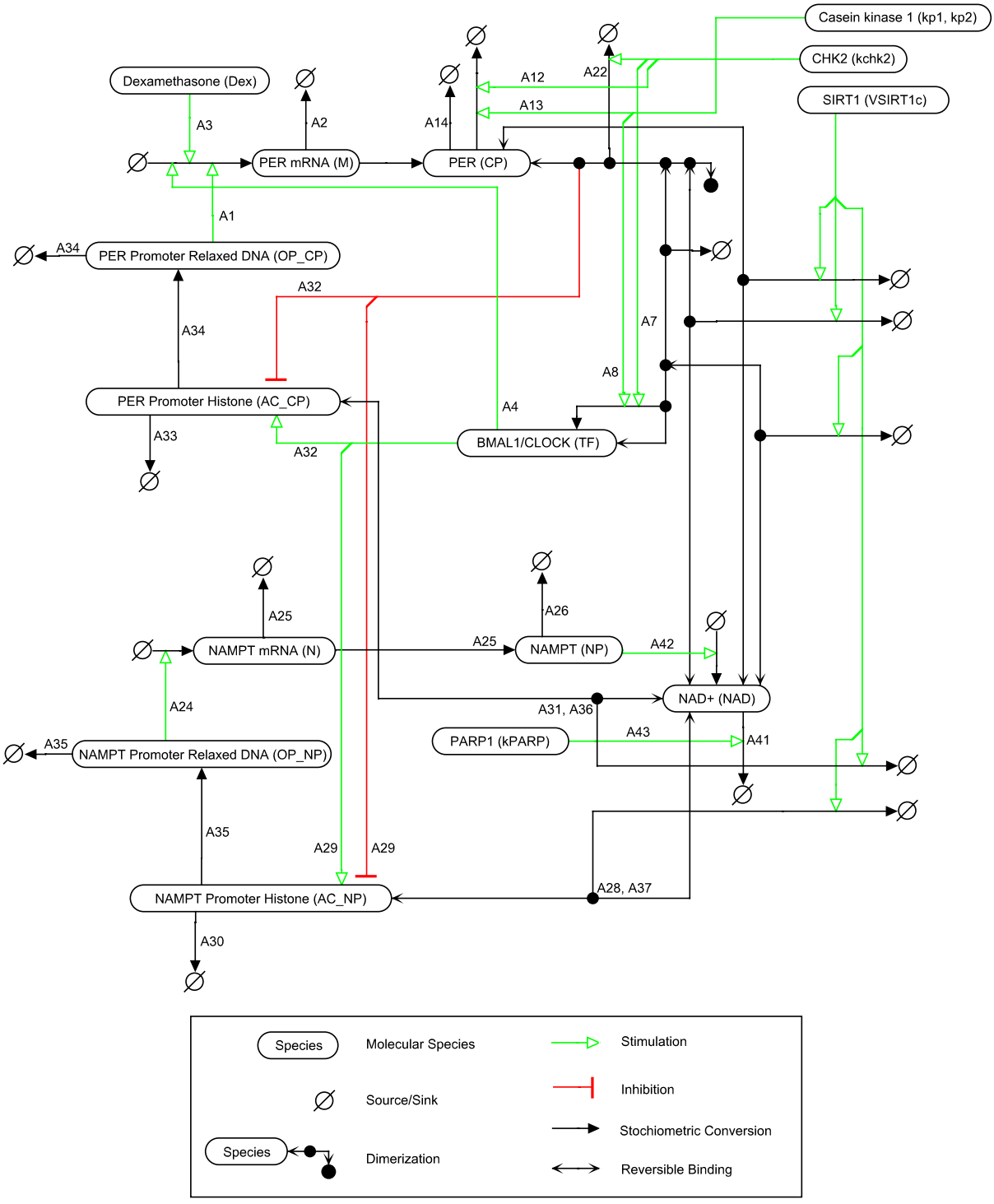

Figure 1: Molecular Interaction Map (MIM) wiring diagram of the simulated system.

Figure 1 shows a wiring diagram for the current model. Each interaction is labelled and described in Table 4; these descriptions are used to label the reactions in the SBML model file.

The original form of CRY/PER mRNA transcription in the Hong 2009 model used a Hill function, but this is zeroed out in the current model using *kms* (*kms=0) in* Equation 1 (below). We extend the Hong 2009 model to account for the effects of acetylation on transcription for both PER and NAMPT by using Equation 1 through Equation 15 from Smolen et al. re-worked for the system described here (Smolen, Hardin et al. 2004). Deacetylation of histones results in chromatin compaction and decreased transcription as a result of lowered accessibility of DNA polymerase to these regions of condensed chromatin. In the case of PER, the first term of Equation 8 accounts for the fractional levels of histone acetylation. The rate of promoter acetylation is a function of acetylation regulated by the BMAL1/CLOCK (TF) complex through CLOCK acetyltransferase activity and inhibited by the effects PER dimer, Equation 13. Further, it is known that CLOCK is able to acetylate histones at positions deacetylated by SIRT1 (Nakahata, Kaluzova et al. 2008). The rate of histone acetylation is regulated by the basal rate of histone deacetylation and the SIRT1 deacetylation, activity simulated as a two substrate Michaelis-Menten reaction that utilizes NAD in the process; the activity of SIRT1 is discussed further below. Therefore, unlike Smolen et al., we do not use a single, fixed deacetylation rate. This is consistent with the work of Nakahata et al., which showed that peak SIRT1 deacetylation activity coincided with the lowest acetylation levels of histone H3 (Nakahata, Kaluzova et al. 2008). This level of single histone acetylation is then used to generate an overall promoter accessibility value, Equation 9. Lastly, this promoter accessibility value is multiplied by a maximal rate of transcription to denote the expression of PER, Equation 1. The same mechanism is used to denote the expression of NAMPT.

Neither SIRT1 expression nor protein levels are under circadian control, yet its deacetylation activity is regulated in a circadian manner (Nakahata, Kaluzova et al. 2008). Therefore, we do not consider changes to SIRT1 levels and only consider the ability of SIRT1 to utilize NAD to deacetylate three species (PER, BMAL1/CLK, and acetylated histone) within the model, thereby affecting circadian rhythms via separate mechanisms. First, SIRT1 deacetylates PER2 destabilizing the protein and promoting its degradation (Asher, Gatfield et al. 2008). Second, acetylation of BMAL1 promotes the binding of CRY1 to BMAL1 and BMAL1 is a target of SIRT1 deacetylation (Grimaldi, Nakahata et al. 2007). Third, as a histone deacetylase SIRT1 is able to deacetylate lysine residues of histones helping to produce transcriptionally silenced chromatin that exists with a closed chromatin structure (Blander and Guarente 2004). Two parameters specify the activity of SIRT1 in the model. The first parameter VSIRT1c regulates the deacetylation of PER (either monomer, dimer, or in complex with BMAL1/CLOCK) and the second parameter, VSIRT1d, regulates the histone deacetylation. The levels of NAD production are regulated using a first-order reaction dependent on the availability of NAMPT. The model includes perturbation inputs from the Hong 2009 model, dexamethosone (*Dex*) and the CHK2 phosphorylation (*kchk2* affecting PER monomer and dimer and *kchk2c* affecting PER in complex with BMAL1/CLOCK).

Kinetic Equations

The model is a system of 11 equations described above and shown below. Equation 12 and Equation 13 denote the rate promoter acetylation for the NAMPT and PER promoters, respectively. Equation 14 denotes the level of inactive complex, while Equation 15 is the total amount of PER that exists in the system.

Equation 1: CRY/PER mRNA

$$\frac{dM}{dt} = VM \cdot OP_{CP} - k_{md} \cdot M + Dex + \frac{k_{ms} \cdot TF^n}{J^n + TF^n}$$

Equation 2: BMAL1/CLOCK complex

$$\frac{dTF}{dt} = -k_{ica}CP2 \cdot TF + \frac{k_{p2}IC}{J_p + CP_{tot}} + k_{chk2c} \cdot IC + k_{cp2d}IC + k_{icd}IC - \frac{V_{SIRT1c}IC \cdot NAD}{k_{aCPSIRT1} \cdot k_{bCPSIRT1} + k_{bCPSIRT1} \cdot IC + IC \cdot NAD}$$

Equation 3: CRY/PER protein monomer

$$\frac{dCP}{dt} = -\frac{V_{SIRT1c}CP \cdot NAD}{k_{aCPSIRT1} \cdot k_{bCPSIRT1} + k_{bCPSIRT1} \cdot CP + CP \cdot NAD} - k_{chk2}CP - \frac{k_{p1} \cdot CP}{J_p + CP_{tot}} + 2k_dCP2 - 2k_aCP \cdot CP - k_{cpd}CP + k_{cps}M$$

Equation 4: CRY/PER protein dimer

$$\frac{dCP2}{dt} = -\frac{V_{SIRT1c}CP2 \cdot NAD}{k_{aCPSIRT1} \cdot k_{bCPSIRT1} + k_{bCPSIRT1} \cdot CP2 + CP2 \cdot NAD} - k_{ica}CP2 \cdot TF - k_{chk2}CP2 - \frac{k_{p2}CP2}{J_p + CP_{tot}} - k_{cp2d}CP2 + k_{icd}IC - k_dCP2 + k_aCP \cdot CP$$

Equation 5: NAMPT mRNA

$$\frac{dN}{dt} = VN \cdot OP_{NP} - k_{nd}N$$

Equation 6: NAMPT protein

$$\frac{dNP}{dt} = -k_{npd}NP + k_{nps}N$$

Equation 7: Single histone acetylation (NAMPT promoter)

$$\frac{dAC_{NP}}{dt} = -\frac{V_{SIRT1d}AC_{NP}NAD}{k_{aCPSIRT1}k_{bCPSIRT1} + k_{bCPSIRT1}AC_{NP} + AC_{NP}NAD} - k_{np_{ac}} * (1 - AC_{NP}) - k_{Np_{deac}} * AC_{NP}$$

Equation 8: Single histone acetylation (CRY/PER promoter)

$$\frac{dAC_{CP}}{dt} = -\frac{V_{SIRT1d}AC_{CP}NAD}{k_{aCPSIRT1}k_{bCPSIRT1} + k_{bCPSIRT1}AC_{CP} + AC_{CP}NAD} + k_{cp_{ac}} * (1 - AC_{CP}) - k_{cp_{deac}} * AC_{CP}$$

Equation 9: DNA Accessibility Value (CRY/PER promoter)

$$\frac{dOP_{CP}}{dt} = \frac{(AC_{CP}{}^{n_{ac}} - OP_{CP})}{T_{const\_cp}}$$

Equation 10: DNA Accessibility Value (NAMPT promoter)

$$\frac{dOP_{NP}}{dt} = \frac{(AC_{NP}{}^{n_{ac}} - OP_{NP})}{T_{const\_np}}$$

Equation 11: NAD

$$\frac{dNAD}{dt} = -\frac{V_{SIRT1d}AC_{CP}NAD}{k_{aCPSIRT1}k_{bCPSIRT1} + k_{bCPSIRT1}AC_{CP} + AC_{CP}NAD} - \frac{V_{SIRT1d}AC_{NP}NAD}{k_{aCPSIRT1}k_{bCPSIRT1} + k_{bCPSIRT1}AC_{NP} + AC_{NP}NAD} - \frac{V_{SIRT1c}IC \cdot NAD}{k_{aCPSIRT1}k_{bCPSIRT1} + k_{bCPSIRT1}IC + IC \cdot NAD} - \frac{V_{SIRT1c}CP2 \cdot NAD}{k_{aCPSIRT1}k_{bCPSIRT1} + k_{bCPSIRT1}CP2 + CP2 \cdot NAD} - \frac{V_{SIRT1c}CP \cdot NAD}{k_{aCPSIRT1}k_{bCPSIRT1} + k_{bCPSIRT1}CP + CP \cdot NAD} - k_{nadd}NAD + VNADc \cdot NP - k_{PARP}NAD$$

Equation 12: Rate of NP promoter acetylation

$$k_{npac} = \frac{TF}{TF + K_{TFNP}} \cdot \frac{K_{CP2NP}}{K_{CP2NP} + CP2}$$

Equation 13: Rate of CP promoter acetylation

$$k_{cpac} = \frac{TF}{TF + K_{TFCP}} \cdot \frac{K_{CP2CP}}{K_{CP2CP} + CP2}$$

Equation 14: Inactive complex (BMAL1/CLOCK and PER dimer)

$$IC = TF_{tot} - TF$$

Equation 15: Total amount of PER

$$CP_{tot} = CP + 2CP2 + 2IC$$

Kinetic parameters

Kinetic parameters used for the current model are described in Table 1; the table also lists the parameter values necessary to reconstitute the Hong 2009 model. Rate constants were based on previously published circadian models (Smolen, Hardin et al. 2004; Hong, Zámborszky et al. 2009). Kinetic parameters unique to the current model were then optimized to generate oscillations in the current work. Rate constants are in units of h^{-1}. The resulting amplitudes have similar orders of magnitude to the original Hong 2009 model.

Initial values

Initial values used in the current model are described in Table 2; initial values to reconstitute the Hong 2009 model are also listed in Table 2. The concentrations of proteins and metabolites are in arbitrary units (AU) because these are currently not known for many circadian clock proteins.

Simulation of DNA damage response

Damage was simulated by altering levels of k_{parp} and k_{chk2} as described in the Results section using the parameters in Table 3.

Period Calculation

The period was calculated by finding the mean of the simulated results and then finding the time points where a selected time point was greater than the mean and the subsequent time point was less than the mean. For each of the selected time points, the previous time point was subtracted to produce the period value. The resulting values were then averaged for the final period value; a requirement was imposed that at least seven oscillations were necessary to produce this value otherwise an error value, negative one, was produced. The period was calculated using the time series for the Cry/Per (CP) protein.

Phase Response Curve (PRC) Calculation

Differences in phase were calculated after 19 days (19 circadian oscillations) between the unperturbed and perturbed systems. The phase shift (advancement or delay) was calculated difference between oscillation peaks for the two systems. Treatments were induced at each circadian hour, and the phase response curve was calculated using the time series data for the Cry/Per (CP) protein.

MATLAB scripts

All simulations were conducted using MATLAB (http://www.mathworks.com). Copies of our model as a Systems Biology Markup Language (SBML) generated using COPASI (http://www.copasi.org) are published as supplemental information on the PLOS One site.

Results

Comparison of Simulated Oscillations to Previous Experimental Results

Figure 2 illustrates the oscillatory behavior simulated by the model using the current parameter set outlined in Table 1. The system oscillates with an autonomous period of 23.8 hours, which is well within the range seen in circadian oscillations of mice (Schwartz and Zimmerman 1990). The current model simulates a free-running circadian clock without external stimuli or cues (zeitgebers) periodically synchronizing the clock and this is the state in which current model results are described. The model can account for entrainment by varying the *Dex* as a square-wave increasing the value of *Dex* to 0.125 for 12 hours and decreasing it to 0 for another 12 hours (not shown). Circadian models, such as the one by Leloup and Goldbeter in 2003, make use of varying PER transcription to simulate the effect of light entrainment. Dexamethasone with its ability to trigger PER transcription therefore is a suitable substitute for entrainment by PER (Leloup and Goldbeter 2003; Reddy, Maywood et al. 2007).

Figure 3 illustrates the oscillations in the histone acetylation levels for both PER and NAMPT mRNA. Histone acetylation levels peak at approximately hour 22 in Figure 3, helping the relaxation of DNA to permit transcription to be initiated. The peak levels of PER and NAMPT mRNA are then reached after a lag of ~6 hours. Experimentally, peaks in the acetylation levels of histones H3 and H4 have been observed 4 and 8 hours in advance of the PER1 and PER2 mRNA peaks (Naruse, Oh-hashi et al. 2004). Acetylated histone and NAD levels oscillate in antiphase, as seen when comparing Figure 3 and Figure 4. This is a feedback mechanism involving NAD production and SIRT1 activity where NAD levels rise to their peak levels ~5 hours after the peak levels of NAMPT mRNA production. This is the time whenSIRT1 activity is at its maximum and acetylated histone levels decline to their minimum ~5 hours later.

NAD levels oscillate by approximately 40% during each circadian cycle, as shown in Figure 4, in response to oscillations in NAMPT protein levels; NAD levels oscillate in phase with NAMPT levels. Similar changes in oscillations levels have been seen experimentally (Nakahata, Sahar et al. 2009; Ramsey, Yoshino et al. 2009). This decline in the NAD levels is a product of several SIRT1 deacetylation processes captured by the current model, as well as the basal degradation of NAD levels via processes external to the model.

Figure 5 shows that the current model retains the phase dynamics present in the Hong 2009 model that are critical in the modeling of circadian systems. There is a lag of ~3 hours between the peak of PER mRNA and the peak in PER monomer levels; this is similar to experimental results seen for mammalian circadian rhythms (Reppert and Weaver 2001). Peaks in the PER monomer levels then proceed prior to the peak in the PER dimer levels several hours later, and peak levels in the PER dimer are then antiphase to the levels of the transcription factor BMAL1/CLOCK.

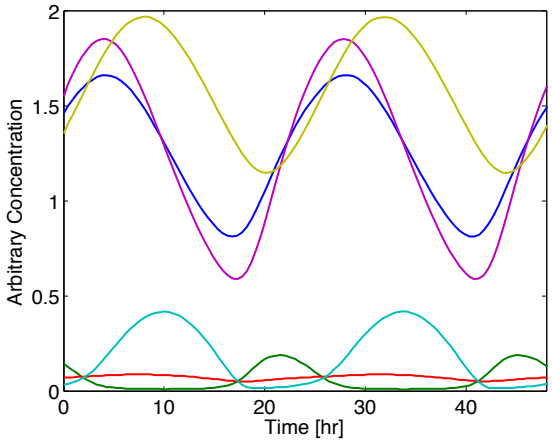

Figure 2: Time series for CRY/PER mRNA (Blue), BMAL1/CLOCK (Green), Cry/Per (Red), Cry/Per Dimer (Cyan), NAMPT mRNA (Purple), NAMPT protein (Yellow). Parameters taken from Table 1 for the current model.

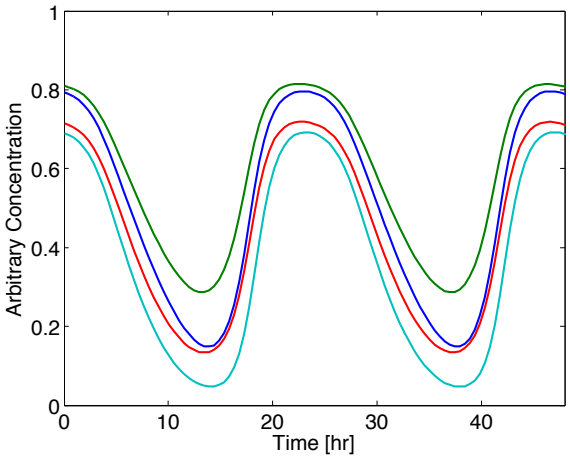

Figure 3: Simulated circadian rhythms of histones and relaxed chromatin. NAMPT acetylated histone levels (Blue), Cry/Per acetylated histone levels (Green), Cry/Per Relaxed Promoter (Red), NAMPT Relaxed Promoter (Cyan). Parameters are from Table 1 for the current model.

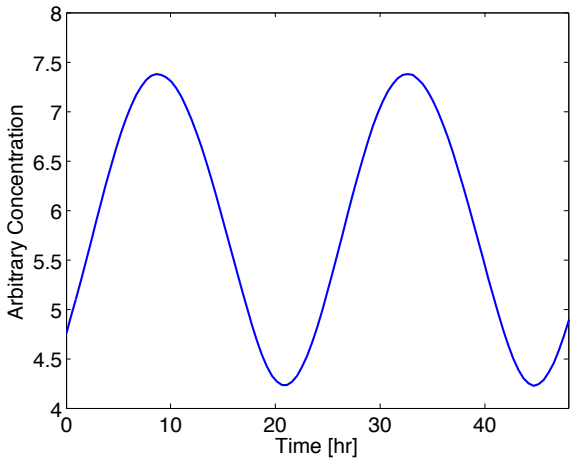

Figure 4: Simulated circadian oscillation of NAD; NAD concentration (Blue). Simulation parameters from Table 1 for the current model.

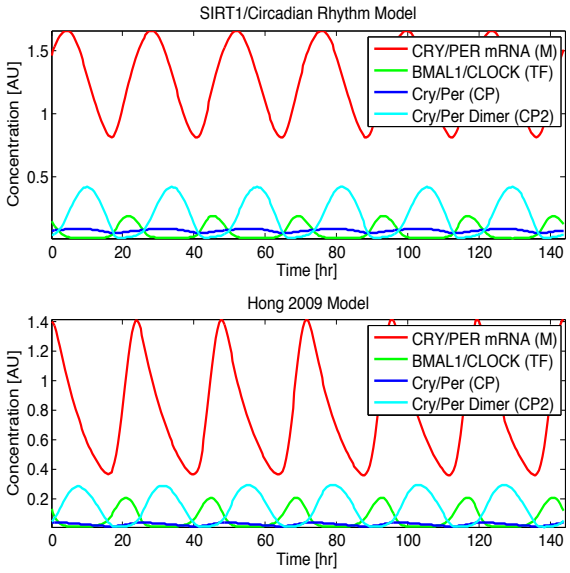

Figure 5: Comparison of current (Top) and Hong 2009 (Bottom) Models. CRY/PER mRNA (Red), BMAL1/CLOCK (Green), CRY/PER protein (Blue), CRY/PER Dimer (Cyan). Only species common to both models are included.

The Hong 2009 model possesses an autocatalytic positive feedback loop involving PER that is a necessary mechanism in order to sustain oscillations (Hong, Zámborszky et al. 2009). This mechanism requires that differential stabilities exist between PER monomer and PER in complexes, either the dimeric form alone or in the dimeric form complexed with BMAL1/CLOCK. This mechanism arises from experimental evidence in the Drosophila circadian clock by Kloss et al. wherein PER complexes where shown to be less susceptible to degradation (Kloss, Price et al. 1998). The current model exhibits the same autocatalytic requirement with a smaller value for the degradation of the PER dimer (*kcp2d)* than for the degradation of the monomeric PER form (*kcpd)* by two magnitudes of order. In contrast to the Hong 2009 model which possesses values for the two parameters (*kcpd* and *kcp2d*) with a smaller difference, we assume the activity of SIRT1 (*VSIRT1c*) in the destabilization of PER in either monomeric or in complexes to be equivalent in the current model, which means that *kcpd2d* accounts for a smaller portion of the degradation of the PER dimer in the current model.

Model Robustness to Parameter Variation

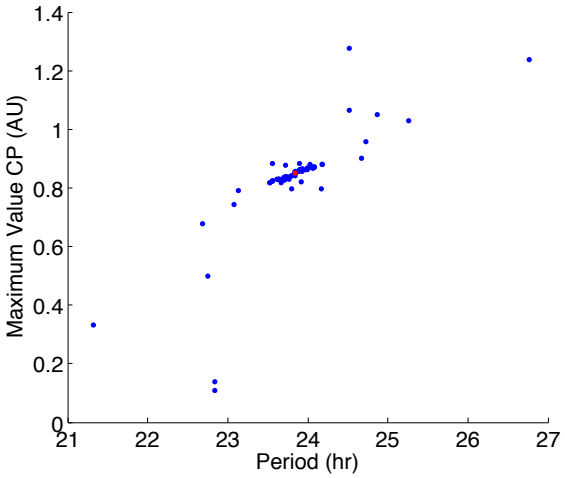

Figure 6: Model robustness as indicated by alterations in amplitude and period. Red: Current model parameter values. Blue: Perturbed parameter values individually increased and decreased by 20%.

Due to the importance of circadian rhythms in the synchronization of biological processes, circadian oscillations must be robust to minor perturbations and must stably oscillate in the presence of varied parameters resulting from individual variation. The results of a study of the circadian rhythms of 72 mice from 12 inbred mouse strains showed this robustness of circadian oscillations (Schwartz and Zimmerman 1990). Across the combined strains, the period mean was 25.53 (range 22.94 to 23.93) hours. We expected a similar robustness in the current model and tested the sensitivity of the model to perturbations of each parameter individually using a method that has been used in computational studies previously (Goldbeter 1995; Smolen, Hardin et al. 2004).

Model robustness was tested by increasing and decreasing parameter values individually by 20% and plotting the resulting amplitudes of PER mRNA (often used as an experimental proxy in PER luciferase experiments) against the oscillation periods. The results of this testing are shown in Figure 6, and this testing suggests that the model is robust to parameter perturbations. Out of the these simulations with perturbations tested none of the parameter sets resulted in periods that deviated from 24 hours by more than 3 hours. A majority of the parameter perturbations clustered near the current model parameter values from Table 1 (this is shown in red in Figure 6) with only slight increases or decreases of the period and amplitude. Stress input variables: *Dex*, *kchk2*, *kchk2c*, and *kPARP* are set to 0 in the current model parameter set, and therefore, they are not expected to, nor did they, have any effect during the sensitivity testing.

Three parameters resulted in periods less than 23 hours and PER mRNA amplitudes less than 0.4 AU. All three of these parameters affected PER, either mRNA or protein, levels. Decreases of 20% to PER protein synthesis rate (*kcps)* and PER mRNA synthesis rate (*VM)*, resulted in this behavior, while an increase of 20% to the PER mRNA degradation *(kmd)* also resulted a similar behavior with a decreased amplitude and period. A 20% decrease in PER mRNA

degradation resulted in the opposite behavior with both an increase in amplitude and a period; as shown in Figure 6, this is the only parameter that resulted in periods greater than 26 hours.

Next, phase response curves (PRCs) were generated using pulses of dexamethasone (*Dex*) which trigger the transcription of PER to draw a comparison with the Hong 2009 model. Phase response curves illustrate the relationship between the timing of a perturbation and the effect of the perturbation on a circadian oscillation is the form of a phase shift (Johnson 1999). There are two types of PRCs, Type 1 and Type 0. The resulting PRC is often dependent on the strength of the perturbation with Type 1 PRCs occurring at lower perturbations that Type 0. At low values of *Dex* (*Dex*=0.15), a Type 1 PRC (shown in Figure 7) is produced whereby there is a continuous transition between phase advancements (positive values on the PRC) and delays (negative values) in response to the dexamethasone stimulus. At high values of *Dex* (*Dex* = 20), a Type 0 PRC is produced with a discontinuity existing between the phase advancements and delays of the system, shown in Figure 8..

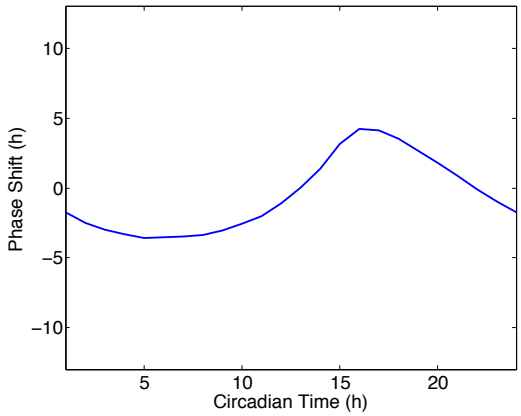

Figure 7: Type 1 PRC.

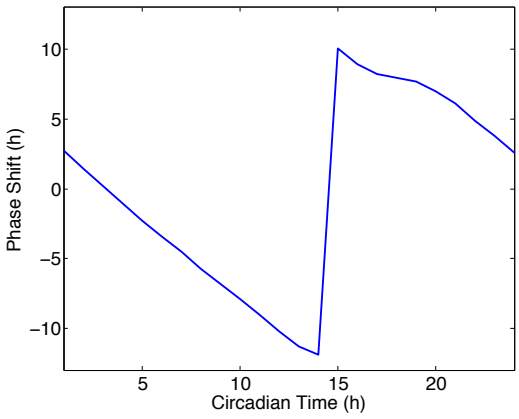

Figure 8: Type 0 PRC.

Effect of NAD Biosynthesis on Circadian Rhythms

Given the multiple interactions in the current model utilizing NAD via SIRT1 deacetylation activity, we next examined the role of NAD biosynthesis. Experimentally, Nakahata et al. inhibited the activity of NAMPT using the pharmacological NAMPT inhibitor FK866 (Nakahata, Kaluzova et al. 2008). Inhibition of NAMPT function resulted in the advancement of peak PER mRNA levels by approximately 3 to 4 hours. The current parameter values from Table 1 were perturbed to simulate decreases in NAD biosynthesis as shown in Figure 9; this inhibition of NAMPT functionality was simulated by the reduction of NAD synthesis (*VNADc*) leading to a decrease in the period. At half the NAD synthesis rate, the period is reduced by one hour, which is qualitatively consistent with the experimentally observed behavior as decreases in the period would advance the circadian oscillations. At values less than 20% of the current value of *VNADc* in Table 1, the circadian oscillations become damped and the period could no longer be calculated; see section Period Calculation for more information. The reason for this dampening can be seen by comparing Figure 10 and Figure 11 which illustrate the rates of concentration change for the BMAL1/CLOCK, PER monomer, PER dimer, and NAD. Figure 10 illustrates that sharp increases in NAD levels are necessary to restore the levels of NAD during each circadian oscillation. The figure also shows that the PER monomer is under tight regulation as an effect of the aforementioned increased stability of the PER dimer with respect to the PER monomer due to their differential degradation rates. NAD levels peak prior to peak PER dimer levels in Figure 10. Both of these properties are opposed in Figure 11. Due to the lower availability of NAD in the system, SIRT1 is less effective at degrading the PER dimer. One predicted effect of this is that PER dimer levels peak prior to NAD levels to further reinforce this dampening behavior in subsequent oscillations.

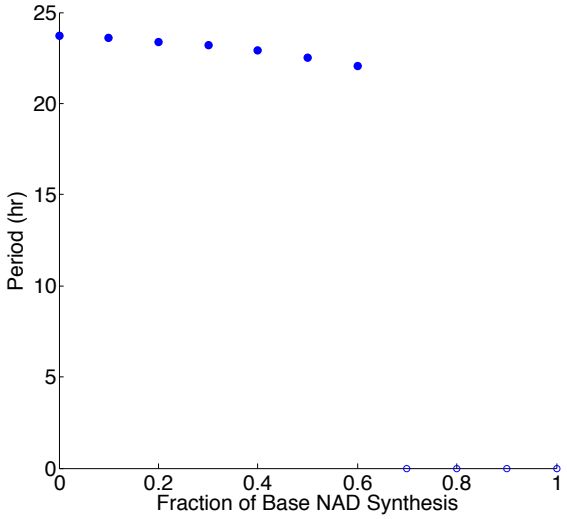

Figure 9: Effect of decreasing NAD biosynthesis on circadian period. Filled circles indicate a period could be determined, unfilled circles indicate that a period could not be determined; refer to Period Calculation for further details.

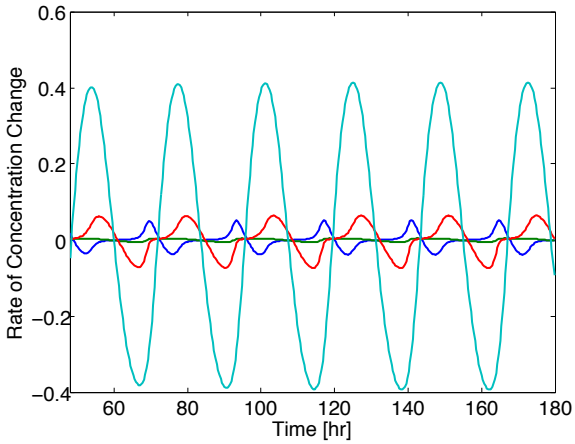

Figure 10: Rate of concentration change using current parameters. Blue: BMAL1/CLOCK (TF), Green: Cry/Per (CP), Red: Cry/Per Dimer (CP2), Cyan: NAD+ (NAD).

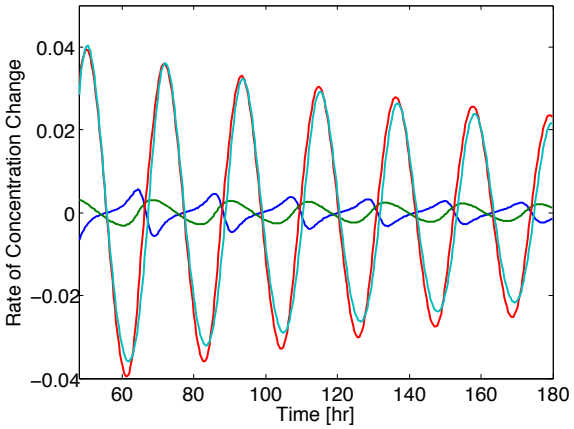

Figure 11: Rate of concentration changes using VNADc at 20% of current parameter. Blue: BMAL1/CLOCK (TF), Green: Cry/Per (CP), Red: Cry/Per Dimer (CP2), Cyan: NAD+ (NAD).

Simulating the Effect of DNA Damage on Circadian Rhythms

Next, we examined the effect of DNA damage on circadian rhythms via the two possible mechanisms that exist in the current model. First, the current model allows the examination of DNA damage as simulated by the activation of CHK2 (*kchk2*) to phosphorylate PER monomer and dimer that triggers their degradation, and the second being sharp decreases in NAD levels on the circadian clock using changes in *kPARP* to simulate PARP1 activity. As a major participant in DNA damage response, PARP1 activity becomes greatly increased in response to DNA strand breaks and is recruited to the sites of DNA damage in a matter of minutes (D'Amours, Desnoyers et al. 1999). Since ionizing radiation results primarily in phase

advancement, we asked whether perturbations in PARP1, singly or in combination with CHK2, could produce similar phase responses, and if so by what mechanism these phase advancements arise.

To compare the phase responses between simulations, we use the measure applied by Hong et al.,which is to take the ratio of the maximum phase advancement in a PRC to the maximum phase delay in the PRC (Hong, Zámborszky et al. 2009). Table 3 shows these PRC ratio results for both the Hong 2009 model using the current model and re-parameterized (using the parameters from Table 1) and for the current model under various parameter conditions. With the re-parameterized model, we first perturb the model using the same *kchk2* (*kchk2*=0.2) from Hong et al. (There is a discrepancy in values for the ratio (3.54 as originally published versus 3.0193 here), but we believe these may be a by-product of numerical analysis and we use our value as the point of comparison.) Perturbing the current model using the same *kchk2* (*kchk2*=0.2) value increases the advance-delay ratio. The ratio is increased because the maximum delay magnitude is decreased by a larger percentage than the maximum advance magnitude.

We next calculated the advance-delay ratio using only *kPARP* (*kPARP*=20) for a treatment duration of two hours. This yielded a ratio result similar to the one observed for the re-implemented Hong 2009 model, 3.0070 versus 3.0193, respectively. We next wondered whether a combination of perturbations would yield higher advance-delay ratio values. Using the values kchk2=0.1 and kparp=20, we calculated a ratio value slightly greater than the ratio value for the CHK2 perturbation alone in the current model, 7.6845 versus 7.5161, respectively. This is with a CHK2 value of half the value used for the Hong 2009 re-parameterization. If we increase the value of *kchk2* to 0.2, we produce a ratio value that is larger 22.6498 and has a near bimodal appearance; numerically, this is caused by a decrease in the magnitude of the maximum delay. Within the context of the model this effect has a direct relation on the activities of SIRT1 in the model both as an inhibitor of transcription and as a mechanism for the destabilization of PER protein. This effect of this CHK2 perturbation occurs at a circadian time of 10 hours, shown in Figure 12, which is during peak of PER dimer levels (the dominant form of the repressor in the system), shown in Figure 2. This degradation allows mRNA levels of PER and NAMPT to rise in advance of the current model thereby resulting in a strong phase advancement. The lowest values for this CHK2-dependent PRC occur at troughs of PER dimer levels. This degradation of the PER dimer repressor causes a slight increase in PER mRNA relative to the current model in the subsequent circadian cycle resulting in the delay observed in the CHK2-dependent PRC.

The CHK2-dependent PRC is in contrast to the PARP-dependent PRC, shown in Figure 12, at the highest value tested (*kparp*=20). At this value, a Type 1 PRC is also produced, but whereas the CHK2 perturbation degrades PER dimer levels, the simulated consumption of NAD by PARP removes an inhibitory effect (the deacetylation of PER by the activity of SIRT1) on this repressor causing an opposite effect; the peak of the PARP-dependent PRC occurs at roughly circadian time 20 hours and its trough at circadian time 10 hours. Therefore, these two perturbations, NAD depletion and PER degradation, may have have different effects depending on the circadian time. The disparate effects of these two perturbations are seen in Figure 12;

advance-delay ratio results are listed in Table 3. In combinations of the two perturbations, a bimodality in the PRC emerges at larger values of the two perturbations, which is not directly seen experimentally in the observations by Oklejewicz et al. suggesting that if this is a mechanism that exists biologically, then the balance between these two forms of perturbation may be under additional regulation (Oklejewicz, Destici et al. 2008). Yet, the phase response curves seen experimentally, as in the case of Oklejewicz et al., in response to DNA damage are undoubtedly the products of several forms of perturbation each that may have a dominant effect depending on the phase of the system during perturbation.

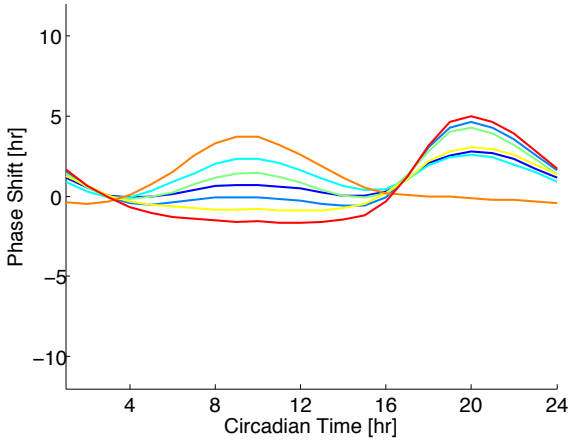

Figure 12: PRCs for various parameter combinations of kchk2 and kparp. Blue: Advance to Delay Ratio: 45.7412; Light Blue: Ratio: 7.6848; Cyan: Ratio: 30.1066; Green: 22.6498; Yellow: Ratio: 3.3353; Orange: Ratio: 7.5161; Red: Ratio: 3.007. Details on parameter values used are found in Table 3.

Discussion/Conclusions

As the underlying mechanisms regulating the circadian clock become better understood (e.g., regarding the effects of other post-translation modifications, such as acetylation, sumolyation, and ubiqutination), these factors could be added to added to the models and possibly related to biological processes.

Here we have developed a simple model that expands on the work of both Hong et al. and Smolen et al. to produce a mathematical model that connects circadian rhythms to DNA damage response and metabolism via the regulation of chromatin remodeling (Smolen, Hardin et al. 2004; Hong, Zámborszky et al. 2009). This model predicts a molecular mechanism through which multiple forms of perturbation, as a result of DNA damage, and multiple post-translational modifications can reproduce an experimentally observed phase response curve PRC. We began with the hypothesis that the activities of SIRT1 and PARP1 in regulating the circadian rhythm could have an impact on the primarily phase advancement behavior seen in circadian oscillations during the response to genotoxic stress given their known interactions with core circadian clock components. To investigate this question, we expanded a previous model to account for the activity of SIRT1 in the regulation of transcription and circadian clock

components and the activity of PARP1 during DNA damage response. The model reveals that the regulation of the circadian clock may be wired in a way that integrates multiple forms post-translational modifications as a mechanism to respond to environmental stress; in the case of acetylation, this post-transcriptional modification is controlled using a circadian feedback mechanism through regulation of NAMPT. We examined phase response curves resulting from various conditions; we did this by using the simulated effects of CHK2 and PARP1 activity. The results of our *in silico* study help to confirm the potential for CHK2 involvement in producing the experimentally observed PRC in the presence of an autocatalytic positive loop regulating PER. These findings are expanded to suggest that NAD depletion via PARP1 activity can produce a similar PRC result as that observed through the removal of the SIRT1 inhibitory effect, and, moreover raising the possibility, that combinations of the two perturbations can also yield a similar effect. These results suggest that multiple perturbations may work in concert to produce the observed PRC.

One part of this system that obviously remains to be explored through a more comprehensive model would include a more complete description of the salvaging of NAD, including the activity of NMNAT1 that yields an intermediate step in this process. Although, NAMPT is the rate-limiting step in the salvage process, it catalyzes the first step in the conversion of nicotinamide (the by-product of SIRT1 and PARP1 catalysis) into nicotinamide mononucleotide; a substrate that is subsequently converted into NAD by NMNAT1 (Rongvaux, Andris et al. 2003). In the current model, only NAMPT has been included, 0because it is under circadian control, and because it is known to be rate limiting in the production of NAD. Yet several publications have shown that SIRT1 can bind to nicotinamide mononucleotide adenylyltransferase 1 (NMNAT1), and it has been hypothesized that this activity may help to stimulate SIRT1 activity (Zhang, Berrocal et al. 2009). This would be an interesting next step to pursue, as well as the more detailed PARP1 dynamics that account for the negative feedback cycle in these dynamics due to its auto-modification capability (D'Amours, Desnoyers et al. 1999).

Supporting Information

Parameter	Description	Current Model	Hong 2009
Dex	Rate of CRY/PER mRNA synthesis by dexamethasone	0	0
k_{ms}	Rate of CRY/PER mRNA synthesis	0	1
J	Michaelis constant for BMAL1/CLOCK binding to CRY/PER promoter	0	0.3
k_{md}	Rate of CRY/PER mRNA degradation	0.13857	0.1
k_{cps}	Rate of CRY/PER protein synthesis	0.40453	0.5
k_{cpd}	Rate of CRY/PER protein degradation	0.48936	0.525
k_a	Rate of CRY/PER dimer association	49.9712	100
k_d	Rate of CRY/PER dimer disassociation	0.36005	0.01
k_{p1}	Rate for monomer phosphorylation	9.4531	10
J_p	Michaelis constant of protein kinase (Casein Kinase 1 Epsilon, CSNK1E)	77.9254	0.05
k_{chk2}	Rate of phosphorylation by CHK2	0	0

k_{icd}	Rate of inactive complex (BMAL1/CLOCK/(CRY/PER)/(CRY/PER)) degradation	0	0.01
k_{cp2d}	Rate of CRY/PER dimer degradation	0.0025	0.0525
k_{ica}	Rate of inactive complex association	28.178	20
k_{chk2c}	Rate of phosphorylation by CHK2	0	0
k_{p2}	Rate for dimer phosphorylation	0.36296	0.1
Tf_{tot}	Total amount of BMAL1/CLOCK	0.84792	0.5
K_{TFCP}	Binding affinity of BMAL1/CLOCK to CRY/PER promoter	0.020133	0
K_{CP2CP}	Binding affinity of CRY/PER dimer to CRY/PER promoter	0.20757	0
K_{TFNP}	Binding affinity of BMAL1/CLOCK to NAMPT promoter	0.040267	0
K_{CP2NP}	Binding affinity of CRY/PER dimer to NAMPT promoter	0.21591	0
k_{cpdeac}	Rate of CRY/PER promoter deacetylation	0.099	0
k_{npdeac}	Rate of NAMPT promoter deacetylation	0.098073	0
VM	Rate of CRY/PER expression	0.40053	0
VN	Rate of NAMPT expression	0.56383	0
n	Hill coefficient for CRY/PER mRNA synthesis	5.1858	2
n_{ac}	Value used to describe the steady state values for promoter accessibility	1.6107	0
T_{const_np}	Time constant for the relaxation of NAMPT promoter to steady state value (AC_NP^n_ac)	0.26014	1
T_{const_cp}	Time constant for the relaxation of CRY/PER promoter to steady state value (AC_NP^n_{ac})	0.22107	1
VSIRT1c	Rate of SIRT1 activity	0.094568	0
k_{nadd}	Rate of NAD+ degradation	1.3309	0
k_{nd}	Rate of NAMPT mRNA degradation	0.16337	0
k_{nps}	Rate of NAMPT protein synthesis	0.20238	0
k_{npd}	Rate of NAMPT protein degradation	0.16024	0
VNADc	Rate of NAD+ production	5.2479	0
$k_{aCPSIRT1}$	Disassociation constant of SIRT1 and NAD+ (Used with non-histone-related equations)	0.10491	0
$k_{bCPSIRT1}$	Michaelis constant for non-histone substrates	0.098395	0
k_{PARP}	Rate of PARP1 activity	0	0
VSIRT1d	Rate of SIRT1 activity	0.070926	0

Table 1: Parameter values for Base and Hong 2009 Model.

Species	Description	Current Model	Hong 2009 Model
M	CRY/PER mRNA	1.4	1.4
TF	BMAL1/CLOCK complex	0.13	0.13
CP	CRY/PER protein	0.037	0.037
CP2	CRY/PER dimer	0.046	0.046
N	NAMPT mRNA	1.5	1.5
NP	NAMPT protein	1	1
AC_{NP}	Single histone acetylation (NAMPT promoter)	0	0.01
AC_{CP}	Single histone acetylation (CRY/PER promoter)	0	0.01
OP_{CP}	DNA Accessibility Value (CRY/PER promoter)	0	0
OP_{NP}	DNA Accessibility Value (NAMPT promoter)	0	0
NAD	NAD+	3	3

Table 2: Initial values for the current and the Hong 2009 Model

Model	kchk2 Value	kparp Value	Maximum Delay (hr)	Maximum Advance (hr)	Advance to Delay Ratio
Hong 2009	0.2	0	-1.6766	5.0623	3.0193
Base Model	0.2	0	-0.4922	3.6996	7.5161
Base Model	0	10	-0.9123	3.0428	3.3353
Base Model	0	20	-1.6618	4.9971	3.0070
Base Model	0.1	10	-0.0612	2.7985	45.7412
Base Model	0.1	20	-0.6026	4.6307	7.6845
Base Model	0.2	10	-0.0848	2.5542	30.1066
Base Model	0.2	20	-0.1883	4.2642	22.6498

Table 3: Results for the analysis of phase shifting behavior by variable kparp.

MIM Annotation	Description	Equation
A1	CP mRNA synthesis (OP_{CP})	1
A2	CP mRNA degradation	1
A3	CP mRNA synthesis (Dex induction)	1
A4	CP mRNA synthesis (TF)	1
A5	IC association	2
A6	IC degradation (phosphorylation)	2

A7	IC degradation (CHK2)	2
A8	IC degradation	2
A9	IC disassociation	2
A10	IC degradation (NAD)	2
A11	CP degradation (NAD)	3
A12	CP degradation (CHK2)	3
A13	CP degradation (phosphorylation)	3
A14	CP degradation	3
A15	CP synthesis	3
A16	CP2 degradation (NAD)	4
A17	IC association	4
A18	CP2 degradation (CHK2)	4
A19	CP2 degradation (phosphorylation)	4
A20	IC degradation	4
A21	IC disassociation	4
A22	CP2 disassociation	4
A23	CP dimerization	4
A24	N mRNA synthesis (OP_{NP})	5
A25	N degradation	5
A26	NP degradation	6
A27	NP synthesis	6
A28	NP acetylated histone deacetylation (NAD)	7
A29	AC_{NP} histone acetylation	7
A30	NP acetylated histone deacetylation	7
A31	CP acetylated histone deacetylation (NAD)	8

A32	AC_{CP} histone acetylation	8
A33	CP acetylated histone deacetylation	8
A34	OP_{CP} synthesis	9
A35	OP_NP synthesis	10
A36	CP acetylated histone deacetylation (NAD)	11
A37	NP acetylated histone deacetylation (NAD)	11
A38	IC degradation (NAD)	11
A39	CP2 degradation (NAD)	11
A40	CP degradation (NAD)	11
A41	NAD degradation	11
A42	NAD synthesis	11
A43	NAD degradation (PARP1)	11
A44	CP2 disassociation	3
A45	CP dimerization	3

Table 4: Description of MIM wiring diagram and connection to model equations. The description column contains species labels from Table 2; IC refers to the "inactive complex" from Equation 14.

Acknowledgements

We thank Sohyoung Kim, Vinodh Rajapakse, and Sudhir Varma for useful discussions.

Funding

This project was funded by the Intramural Research Program of the National Institutes of Health; Center for Cancer Research; National Cancer Institute.

References

Asher, G., D. Gatfield, et al. (2008). "SIRT1 regulates circadian clock gene expression through PER2 deacetylation." Cell **134**(2): 317-328.

Blander, G. and L. Guarente (2004). "The Sir2 family of protein deacetylases." Annu Rev Biochem **73**: 417-435.

D'Amours, D., S. Desnoyers, et al. (1999). "Poly(ADP-ribosyl)ation reactions in the regulation of nuclear functions." Biochem J **342 (Pt 2)**: 249-268.

de Murcia, J. M., C. Niedergang, et al. (1997). "Requirement of poly(ADP-ribose) polymerase in recovery from DNA damage in mice and in cells." Proc Natl Acad Sci U S A **94**(14): 7303-7307.

Doi, M., J. Hirayama, et al. (2006). "Circadian regulator CLOCK is a histone acetyltransferase." Cell **125**(3): 497-508.

Eide, E. J., M. F. Woolf, et al. (2005). "Control of mammalian circadian rhythm by CKIepsilon-regulated proteasome-mediated PER2 degradation." Mol Cell Biol **25**(7): 2795-2807.

Engelen, E., R. C. Janssens, et al. (2013). "Mammalian TIMELESS Is Involved in Period Determination and DNA Damage-Dependent Phase Advancing of the Circadian Clock." PloS one **8**(2): e56623.

Gallego, M., E. J. Eide, et al. (2006). "An opposite role for tau in circadian rhythms revealed by mathematical modeling." Proc Natl Acad Sci U S A **103**(28): 10618-10623.

Gery, S., N. Komatsu, et al. (2006). "The circadian gene per1 plays an important role in cell growth and DNA damage control in human cancer cells." Mol Cell **22**(3): 375-382.

Goldbeter, A. (1995). "A model for circadian oscillations in the Drosophila period protein (PER)." Proc Biol Sci **261**(1362): 319-324.

Gonze, D., J. Halloy, et al. (2002). "Robustness of circadian rhythms with respect to molecular noise." Proc Natl Acad Sci U S A **99**(2): 673-678.

Grimaldi, B., Y. Nakahata, et al. (2007). "Chromatin remodeling and circadian control: master regulator CLOCK is an enzyme." Cold Spring Harb Symp Quant Biol **72**: 105-112.

Hirayama, J., S. Sahar, et al. (2007). "CLOCK-mediated acetylation of BMAL1 controls circadian function." Nature **450**(7172): 1086-1090.

Hong, C. I., J. Zámborszky, et al. (2009). "Minimum criteria for DNA damage-induced phase advances in circadian rhythms." PLoS computational biology **5**: e1000384.

Izumo, M., T. R. Sato, et al. (2006). "Quantitative analyses of circadian gene expression in mammalian cell cultures." PLoS Comput Biol **2**(10): e136.

Johnson, C. H. (1999). "Forty years of PRCs--what have we learned?" Chronobiol Int **16**(6): 711-743.

Kloss, B., J. L. Price, et al. (1998). "The Drosophila clock gene double-time encodes a protein closely related to human casein kinase Iepsilon." Cell **94**(1): 97-107.

Koh, D. W., T. M. Dawson, et al. (2005). "Mediation of cell death by poly(ADP-ribose) polymerase-1." Pharmacological research : the official journal of the Italian Pharmacological Society **52**: 5-14.

Kwon, H. S. and M. Ott (2008). "The ups and downs of SIRT1." Trends Biochem Sci **33**(11): 517-525.

Leloup, J. C. and A. Goldbeter (2003). "Toward a detailed computational model for the mammalian circadian clock." Proc Natl Acad Sci U S A **100**(12): 7051-7056.

Leonardi, G. C., V. Rapisarda, et al. (2012). "Correlation of the risk of breast cancer and disruption of the circadian rhythm (Review)." Oncol Rep **28**(2): 418-428.

Levi, F., A. Okyar, et al. (2010). "Circadian timing in cancer treatments." Annu Rev Pharmacol Toxicol **50**: 377-421.

Mormont, M. C. and F. Levi (1997). "Circadian-system alterations during cancer processes: a review." Int J Cancer **70**(2): 241-247.

Nakahata, Y., M. Kaluzova, et al. (2008). "The NAD+-dependent deacetylase SIRT1 modulates CLOCK-mediated chromatin remodeling and circadian control." Cell **134**(2): 329-340.

Nakahata, Y., S. Sahar, et al. (2009). "Circadian control of the NAD+ salvage pathway by CLOCK-SIRT1." Science **324**(5927): 654-657.

Naruse, Y., K. Oh-hashi, et al. (2004). "Circadian and light-induced transcription of clock gene Per1 depends on histone acetylation and deacetylation." Mol Cell Biol **24**(14): 6278-6287.

Oklejewicz, M., E. Destici, et al. (2008). "Phase resetting of the mammalian circadian clock by DNA damage." Curr Biol **18**(4): 286-291.

Pregueiro, A. M., Q. Liu, et al. (2006). "The Neurospora checkpoint kinase 2: a regulatory link between the circadian and cell cycles." Science **313**(5787): 644-649.

Ptitsyn, A. A. and J. M. Gimble (2011). "True or false: all genes are rhythmic." Ann Med **43**(1): 1-12.

Ramsey, K. M., J. Yoshino, et al. (2009). "Circadian clock feedback cycle through NAMPT-mediated NAD+ biosynthesis." Science **324**(5927): 651-654.

Rana, S. and S. Mahmood (2010). "Circadian rhythm and its role in malignancy." J Circadian Rhythms **8**: 3.

Reddy, A. B., E. S. Maywood, et al. (2007). "Glucocorticoid signaling synchronizes the liver circadian transcriptome." Hepatology **45**(6): 1478-1488.

Reppert, S. M. and D. R. Weaver (2001). "Molecular analysis of mammalian circadian rhythms." Annu Rev Physiol **63**: 647-676.

Rongvaux, A., F. Andris, et al. (2003). "Reconstructing eukaryotic NAD metabolism." Bioessays **25**(7): 683-690.

Schwartz, W. J. and P. Zimmerman (1990). "Circadian timekeeping in BALB/c and C57BL/6 inbred mouse strains." J Neurosci **10**(11): 3685-3694.

Smolen, P., P. E. Hardin, et al. (2004). "Simulation of Drosophila circadian oscillations, mutations, and light responses by a model with VRI, PDP-1, and CLK." Biophysical journal **86**: 2786-2802.

Zhang, T., J. G. Berrocal, et al. (2009). "Enzymes in the NAD+ salvage pathway regulate SIRT1 activity at target gene promoters." J Biol Chem **284**(30): 20408-20417.